PROCEEDINGS, Thirty-Fifth Workshop on Geothermal Reservoir Engineering
Stanford University, Stanford, California, February 1-3, 2010
SGP-TR-188

REACTIVE FLOW IN A NATURAL FRACTURE IN PORO-THERMO-ELASTIC ROCK

C. Rawal and A. Ghassemi

Harold Vance Department of Petroleum Engineering
3116 TAMU
College Station, TX, 77843, USA
e-mail: ahmad.ghassemi@pe.tamu.edu
chakra.rawal@pe.tamu.edu

ABSTRACT

Poro-thermo-mechanical processes and mineral precipitation/dissolution change the fracture aperture and thus affect the fluid flow pattern in the fracture. In this paper, we study this phenomenon by further development and application of a three-dimensional thermo-poro-mechanical model to include silica dissolution-precipitation effects. The solid mechanics aspect of the problem is treated using poro-thermo-elastic displacement discontinuity method (Ghassemi et al., 2007; Ghassemi and Zhou, 2009), while reactive flow and heat transport in the fracture is solved using finite element method. We focus on single component reactive fluid transport in a fracture (Tang et al., 1981; Steefel and Lichtner, 1998; Wangen and Munz, 2004; Ghassemi and Kumar, 2005). Solute reactivity along the fracture plane is considered using temperature dependent reaction kinetics. We apply the model to simulate the impact of cold water circulation on the dynamics of fracture permeability in enhanced geothermal system.

INTRODUCTION

In extraction of thermal energy from hot-reservoir-rocks, the fluid flows through natural fractures in the reservoirs. This circulation of low-temperature fluid in fractures leads to the variation in the geometry of fractures which can be described as its response to mechanical, thermal and chemical processes. Different aspects of thermal and mechanical processes have been studied by researchers (e.g. Ghassemi and Zhang, 2004; Ghassemi and Kumar, 2005, 2007; Ghassemi et al., 2003, 2007; Ghassemi and Zhou, 2009). The thermo-elastic effects are reported dominant near the injection when compared to those of poro-elasticity and under some conditions, silica reactivity may dominate permeability (Ghassemi and Kumar, 2007). Furthermore, experimental studies (Carroll et al., 1998; Johnson et al., 1998; Dobson et al., 2003) also show that chemical precipitation and dissolution of minerals significantly affect fracture aperture.

In general, simulating poro-thermo-elastic-chemical mechanisms involves solving a set of equations each for fluid flow, heat transport, solute transport/reactions and elastic response of the reservoir and more importantly, these processes are generally coupled. In present work, we use a partially coupled poro-thermo-elastic approach (Ghassemi and Zhou, 2009) and the *displacement discontinuity method* (e.g. Ghassemi et al., 2007) to simulate the poro-mechanical processes. On the other hand, we fully couple reactive flow and heat transport in the fracture and use the *finite element method* to find a solution for their distributions within the fracture. Currently, we only focus on single-component mineral reaction and its transport in the fracture. The solute reactivity and solubility in fracture plane is considered using a temperature dependent formulation (e.g., Robinson, 1982; Rimstidt and Barnes, 1980).

GOVERNING EQUATIONS

The physical and chemical processes are represented and described by a number of equations that are obtained by consideration of constitutive models, transport, and balance laws (.e.g. fluid momentum, fluid continuity).

Fluid Flow in the fracture and reservoir-matrix

Assuming fluid flow in the fracture as laminar, the conservation of momentum can be written for unknown pressure gradient as (Ghassemi and Zhou, 2009):

$$\nabla p(x,y,0,t) = -\frac{12\mu}{w^3(x,y,t)}\mathrm{q}(x,y,t) \qquad (1)$$

Similarly, with assumption of incompressible fluid, the fluid continuity equation can be expressed as:

$$-\nabla \cdot \mathrm{q}(x,y,t) - 2q_L(x,y,t) = \frac{\partial w(x,y,t)}{\partial t} \qquad (2)$$

Combining Eqs. (1) and (2) leads to:

$$\nabla.\left[\frac{w^3}{12\mu}\nabla p(x,y,0,t)\right] \qquad (3)$$
$$-2q_L(x,y,t) = \frac{\partial w(x,y,t)}{\partial t}$$

where p is the fluid pressure in the fracture, μ is the fluid viscosity; w is the fracture aperture , q is the fluid discharge. Similarly, ∇ and $\nabla\cdot$ are gradient and divergence operators respectively. q_L accounts for the velocity of fluid leaking-off from one side of the fracture to the formation.

The boundary conditions needed to solve Eq. (3) are generally prescribed at the injection and extraction well locations. For example, here the boundary conditions specified are constant injection rate and pressure at the injection and extraction well locations respectively:

$$Q(x_i,y_i,t) = Q_i \qquad (4)$$
$$p(x_e,y_e,t) = P_e$$

Since reservoir rock is permeable so the injectate will leak-off from the fracture or fracture zone into the formation. Using Darcy's law, fluid leak-off velocity can be computed as;

$$q_L(x,y,t) = -\frac{k}{\mu}\frac{\partial p(x,y,z,t)}{\partial n}\bigg|_{z=0} \qquad (5)$$

where k is rock permeability, n is the outward normal of the fracture surface and $z=0$ denotes the fracture surface.

The field-equations for poro-elasticity (Biot, 1941) can be represented as Navier equation with coupling term and a diffusion equation as in (Cheng and Detournay, 1998).

$$G\nabla_2^2 u_i + \left(\frac{G}{1-2\nu}\right)u_{k,ki} - \alpha p_{,i} = 0 \qquad (6)$$

$$\frac{\partial p}{\partial t} - \frac{2\kappa GB^2(1-2\nu)(1+\nu_u)^2}{9(\nu_u-\nu)(1-2\nu_u)}\nabla_3^2 p = -\frac{2GB(1+\nu_u)}{3(1-2\nu_u)}\frac{\partial \varepsilon}{\partial t} \qquad (7)$$

where u_i is the solid displacement in the i direction, p is the pore pressure, G is the shear modulus, ν and ν_u respectively are the drained and un-drained Poisson's ratios, α is the Biot's coefficient of effective stress, B is the Skempton's pore pressure coefficient, ε is the volumetric strain. Here p is used for both pressure in the reservoir matrix and fracture (assuming no filter cake). Initial and boundary conditions for Eqs. (6)-(7) are given as:

$$p(x,y,z,0) = p_0 \qquad (8)$$

$$p(x,y,z,t)\big|_{z=0^+} = p(x,y,0,t) \qquad (9)$$

Heat transfer in the fracture and rock-matrix

Assuming heat transfer by advection due to fluid motion and conduction through the fracture wall, the heat transport equation in the fracture can be written as:

$$\rho_f c_f \mathrm{q}(x,y).\nabla T(x,y,0,t) + q_h(x,y,0,t) = 0 \qquad (10)$$

The heat conduction is represented by its source intensity (q_h), which can be computed using well-known Fourier's law as:

$$q_h(x,y,0,t) = -2K_r\frac{\partial T(x,y,z,t)}{\partial z}\bigg|_{z=0} \qquad (11)$$

where ρ_f is the fluid density, c_f is the specific heat of the fluid and q_h is the heat source intensity and it represents the heat transfer rate between the reservoir matrix and the fracture and K_r is the rock thermal conductivity and T is the temperature.

In low-permeability reservoir matrix where leak-off usually is small, heat conduction, is only the dominant transport mechanism in reservoir matrix and governed by:

$$\frac{\partial T(x,y,z,t)}{\partial t} = \frac{K_r}{\rho_r c_r}\nabla^2 T(x,y,z,t) \qquad (12)$$

where ρ_r is the rock density, c_r is the specific heat of the rock and ∇^2 is the Laplacian operator in three dimensions, and Ω represents the 3D reservoir domain.

The initial and boundary conditions associated with Eqs. (10)-(12) are:

$$T(x,y,z,0) = T^o; T(x_i,y_i,0,t) = T_{inj} \qquad (13)$$

where T^o is the initial rock temperature and T_{inj} is the temperature of the injected fluid. The solution of the thermo-elasticity in 3-D using integral equation formulation is been given detail in (Ghassemi et al., 2003, 2005; Ghassemi and Zhou, 2009).

Solute transport and reactivity

The mineral dissolution and precipitation in geothermal systems can lead to complex scenarios. However, considering reactivity of silica using a

single-component reactive-transport model may be adequate under certain conditions of interest (e.g., Tang et al, 1981, Steefel and Lichtner, 1998; Wangen and Munz, 2004; Ghassemi and Kumar, 2005). In this work, the advection, first order reaction and diffusion of silica in the reservoir matrix are considered as the principal transport mechanisms (as in Ghassemi and Kumar, 2007).

Assuming the fluid and rock characteristics (e.g. diffusivity coefficients, porosity) as constant, the single-component solute transport system considering temperature-dependent both reaction rate and equilibrium concentration (as in Ghassemi and Kumar, 2005) can be expressed in the planar fracture as:

$$\begin{aligned} &\mathrm{q}(x,y).\nabla C(x,y,0,t)+2KC(x,y,0,t) \\ &+q_s(x,y,0,t)=2KC^{ceq} \end{aligned} \tag{14}$$

where C and C^{eq} are the total and equilibrium mineral concentration respectively; K is intrinsic reaction-rate constant(here assumed temperature-dependent only). Similarly, q_s is the solute source intensity and can be written as:

$$q_s(x,y,0,t)=-2\phi D^{'}\left.\frac{\partial C(x,y,z,t)}{\partial z}\right|_{z=0} \tag{15}$$

where $D^{'}$ is *effective* solute diffusion coefficient and ϕ is the porosity of the reservoir matrix. With the assumption of negligible mineral reaction in the reservoir matrix, solute transport in the reservoir matrix is diffusion-dominated and governed as:

$$\frac{\partial C(x,y,z,t)}{\partial t}=D'\nabla_3^2 C(x,y,z,t) \tag{16}$$

The Eqs. (14)-(16) are subjected to the initial and boundary conditions and are summarized :

$$\begin{aligned} &C(x,y,z,0)=C^o \\ &C(x_i,y_i,0,t)=C_{inj} \end{aligned} \tag{17}$$

where C^o is the initial solute concentration (here assumed as equilibrium state) and C_{inj} is the injectate concentration.

NUMERICAL SOLUTION

The system of equations is solved using a combined *finite element* and *boundary element method*. We use the *finite element method* to model fluid flow, heat and solute transport in the fracture surface. In this way only a two-dimensional discretization is required.

Integral Equation Method

In this method, fracture in poroelastic medium is represented as a discontinuity surface, across which displacement, normal fluxes of fluid, heat and solute sources are discontinuous. Importantly, such surface can be computed using the distributions of impulse point discontinuities over time and space. If the so called "density" of a singularity is known, an integral representation of respective field-quantity (e.g. displacement) is possible using the integral equation method. This approach has been used by (Ghassemi and Zhou, 2009) to solve for the stress; pore pressure around fracture. Applying the technique to the system of interest herein, yields:

$$C(\mathbf{x},t)=\int_0^t\int_A \frac{C^{is}(\mathbf{x}-\mathbf{x}',t-t')}{D_s(\mathbf{x}',t')\,dA(\mathbf{x}')dt'}+C^o(\mathbf{x}) \tag{18}$$

$$\begin{aligned} p(\mathbf{x},t)=&\int_0^t\int_A \frac{p_n^{id}(\mathbf{x}-\mathbf{x}',t-t')}{D_n(\mathbf{x}',t')\,dA(\mathbf{x}')}dt' \\ &+\int_0^t\int_A \frac{p^{if}(\mathbf{x}-\mathbf{x}',t-t')}{D_f(\mathbf{x}',t')\,dA(\mathbf{x}')}dt'+p^o(\mathbf{x}) \end{aligned} \tag{19}$$

$$T(\mathbf{x},t)=\int_0^t\int_A \frac{T^{ih}(\mathbf{x}-\mathbf{x}',t-t')}{D_h(\mathbf{x}',t')\,dA(\mathbf{x}')dt'}+T^o(\mathbf{x}) \tag{20}$$

$$\begin{aligned} \sigma_n(\mathbf{x},t)=&\int_0^t\int_A \frac{\sigma_{nn}^{id}(\mathbf{x}-\mathbf{x}',t-t')}{D_n(\mathbf{x}',t')\,dA(\mathbf{x}')}dt' \\ &+\int_0^t\int_A \frac{\sigma_n^{if}(\mathbf{x}-\mathbf{x}',t-t')}{D_f(\mathbf{x}',t')\,dA(\mathbf{x}')}dt' \\ &+\int_0^t\int_A \frac{\sigma_n^{ih}(\mathbf{x}-\mathbf{x}',t-t')}{D_h(\mathbf{x}',t')\,dA(\mathbf{x}')}dt'+\sigma_n^0(\mathbf{x}) \end{aligned} \tag{21}$$

Here t is time, A is the fracture surface, D_s is solute source intensity. Similarly D_n, D_f and D_h are displacement discontinuity and intensity of (fluid and heat sources) respectively. C^{is}; σ_{nn}^{id}, σ_n^{if}, σ_n^{ih}; p_{ij}^{id}; p^{if} and T^{ih} are the instantaneous fundamental solutions of: concentration; incremental stress; pore pressure and temperature due to unit impulse of solute source intensity ("*is*"), displacement discontinuity ("*id*"), the fluid source intensity ("*if*") and the heat source intensity ("*ih*"); and p^o and T^o are initial pore pressure and temperature.

Finite Element Formulation for Fluid flow, heat and solute transport

A conventional Galerkin approach is applied to model the 2D reactive flow and transport in the fracture which is divided into boundary elements as part of the 3D solid mechanics solution. The

following interpolating functions in an element (*m)* (e.g. similar to Ghassemi and Zhou, 2009):

$$C^{(m)} = \mathrm{N}^{(m)}\tilde{\mathbf{C}}, D_s^{(m)} = \mathrm{N}^{(m)}\tilde{\mathbf{D}}_\mathbf{s}$$
$$p^{(m)} = \mathrm{N}^{(m)}\tilde{\mathbf{p}}\ , D_f^{(m)} = \mathrm{N}^{(m)}\tilde{\mathbf{D}}_\mathbf{f} \qquad (22)$$
$$T^{(m)} = \mathrm{N}^{(m)}\tilde{\mathbf{T}}, D_h^{(m)} = \mathrm{N}^{(m)}\tilde{\mathbf{D}}_\mathbf{h}$$

Here m is an element and $\mathrm{N}^{(m)}$ are interpolative functions. Similarly, $\tilde{\mathbf{C}}, \tilde{\mathbf{D}}_\mathbf{s}; \tilde{\mathbf{p}}, \tilde{\mathbf{D}}_\mathbf{f}; \tilde{\mathbf{T}}, \tilde{\mathbf{D}}_\mathbf{h}$ are the vectors of concentration and source intensity (solute); fluid pressure and source intensity (fluid); temperature, source intensity (heat), respectively at the element nodes. Discretization of the governing equations (Eqns. ((3), (10) and(14)) to form stiffness matrices leads to following system of equations respectively:

$$\mathbf{A_1}\tilde{\mathbf{p}}(\mathbf{t}) + \mathbf{A_2}\tilde{\mathbf{D}}_\mathbf{f}(\mathbf{t}) = \mathbf{B_1}(\mathbf{t}) \qquad (23)$$
$$\mathbf{A_3}\tilde{\mathbf{T}}(\mathbf{t}) + \mathbf{A_4}\tilde{\mathbf{D}}_\mathbf{h}(\mathbf{t}) = \mathbf{B_2}(\mathbf{t}) \qquad (24)$$
$$\mathbf{A_5}\tilde{\mathbf{C}}(\mathbf{t}) + \mathbf{A_6}\tilde{\mathbf{D}}_\mathbf{s}(\mathbf{t}) = \mathbf{B_3}(\mathbf{t}) \qquad (25)$$

Entries of the matrices and vectors in Eqns. (23)-(25) are similar to those in (Ghassemi and Zhou, 2009) but have been extended to include reactive flow.

Discretization of Integral Equation

The Integral equations are discretized in spatial domain (using same 'mesh' as in finite element method) and in time domain using convolution algorithm (e.g., Dargush and Banerjee, 1989). For example, if we discretize time (t) into N equal segments (Δt), integral equation for concentration in terms of those in time segments, can be written as:

$$C(\mathbf{x},t) = \left[\sum_{m=1}^{M}\int_{A_e}\mathbf{N}^{(m)}C^{cs}_{(1)}(\mathbf{x}-\mathbf{x}')\,dA(\mathbf{x}')\right]\tilde{\mathbf{D}}_\mathbf{s}(N\Delta t)$$
$$+\sum_{n=1}^{N-1}\left[\sum_{m=1}^{M}\int_{A_e}\mathbf{N}^{(m)}C^{cs}_{(N-n+1)}(\mathbf{x}-\mathbf{x}')\,dA(\mathbf{x}')\right]\tilde{\mathbf{D}}_\mathbf{s}(n\Delta t) + C^0(\mathbf{x}) \qquad (26)$$

where

$$C^{cs}_{(k)}(..) = \begin{cases} C^{cs}(..,\Delta t) & ; k=1 \\ C^{cs}(..,k\Delta t) - C^{cs}(..,(k-1)\Delta t); & k>1 \end{cases}$$

The fundamental solutions for stress, temperature and pressure can be found in (Cheng and Detournay, 1998). The fundamental solution for solute is obtained by analogy with pore pressure source solution. Applying integral equation for stress on element centers while for pore-pressure, temperature and concentration (Eqs.(26)) on all element nodes in the fracture plane, we obtain:

$$\boldsymbol{\sigma}_\mathbf{n} = \mathbf{A_7}\tilde{\mathbf{D}}_\mathbf{n}(\mathbf{t}) + \mathbf{A_8}\tilde{\mathbf{D}}_\mathbf{f}(\mathbf{t}) + \mathbf{A_9}\tilde{\mathbf{D}}_\mathbf{h}(\mathbf{t}) + \boldsymbol{\sigma}_\mathbf{n1} + \boldsymbol{\sigma}_\mathbf{n0} \qquad (27)$$
$$\tilde{\mathbf{p}} = \mathbf{A_{10}}\tilde{\mathbf{D}}_\mathbf{n}(\mathbf{t}) + \mathbf{A_{11}}\tilde{\mathbf{D}}_\mathbf{f}(\mathbf{t}) + \mathbf{p_1} + \mathbf{p^o} \qquad (28)$$
$$\tilde{\mathbf{T}} = \mathbf{A_{12}}\tilde{\mathbf{D}}_\mathbf{h}(\mathbf{t}) + \mathbf{T_1} + \mathbf{T^o} \qquad (29)$$
$$\tilde{\mathbf{C}} = \mathbf{A_{13}}\tilde{\mathbf{D}}_\mathbf{s}(\mathbf{t}) + \mathbf{C_1} + \mathbf{C^o} \qquad (30)$$

Calculation of Fracture aperture change caused by mineral dissolution and precipitation

The fracture aperture change due to silica dissolution and precipitation can be computed using mass balance of mineral that is lost or gained after change in its concentration in the circulating fluid (Robinson and Pendergrass, 1989):

$$w(x,y,0,t) = w_o - \frac{2*10^{-6} f_Q \rho_f K \Delta t}{\rho_Q}\left(C - C^{eq}\right) \qquad (31)$$

where w_o is the initial fracture aperture.

The intrinsic reaction rate constant and equilibrium concentration are given as (Robinson, 1982; Robinson and Pendergrass, 1989):

$$K(T) = 10^{0.433-4090/T}$$
$$c^{eq}(T) = 6\times10^4 \times 10^{1.881-2.028\times10^{-3}T-1560/T} \qquad (32)$$

For each element, the fracture aperture change is estimated by substituting the solved concentration from (Eqn. (25)), and the estimated reaction rate constant and equilibrium concentration (Eqn. (32)) into Eqn. (31). In this calculation, the contributions of the nodal variables to an element (at its center) are approximated using the shape functions.

EXAMPLE CASE

Rectangular Fracture

Consider a 3D geothermal reservoir containing a fracture or a fracture zone that is rectangular (600 m × 180 m). This zone is divided into 1258 four-nodded quadrilateral elements. All the variables (except stress, fluid discharge and fracture aperture which are approximated at the element centers) are computed at elemental nodes. Finite element mesh of the fracture surface is shown in Figure 1.

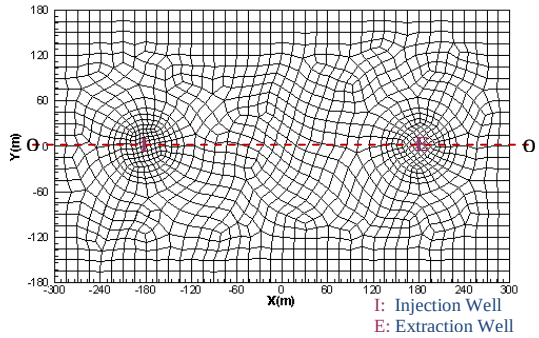

Figure 1: fracture surface mesh with locations of the injection and extraction well

The input parameters are given in *Table 1* below:

Table 1: Input Parameters

Parameter	Value	Units
Q	10	*l/sec*
w_o	50	*μm*
ϕ	1	*%*
υ	0.25	-
α_T	8.0×10^{-6}	K^{-1}
ρ_R	2650	kgm^{-3}
ρ_W	1000	kgm^{-3}
C_R	800	$Jkg^{-}1K^{-1}$
C_W	4200	$Jkg^{-1}K^{-1}$
μ_W	0.001	*Pa-s*
K_R	2.9	$Wm^{-1}K^{-1}$
T_{RO}	523	*K*
T_{Inj}	300	*K*
D'	1.157×10^{-9}	m^2s^{-1}
ρ_Q	2650	kgm^{-3}
f_Q	20	*%*
C_{inj}	100	*ppm*
α	0.47	-
C_D	1.0×10^{-5}	m^2s^{-1}
G	15,000	*MPa*
P_0	17.4	*MPa*
K_n	3×10^{11}	*Pa/m*

Silica dissolution and precipitation

The concentration of injecting fluid in the fracture is 100 ppm and it is assumed that initially the reservoir matrix is at equilibrium state (~ 412 ppm) with respect to silica solubility. Figure 2 show the distribution of the silica concentration in the fracture for injection times of 15 days and 1 year respectively. It is observed that as time increases, the low concentration region originating near injection well extended towards extraction well as silica concentration in the extracting fluid gets decreased (as shown in Figure 4). The variation of the concentration is acute near extraction well.

Fracture aperture change due to Silica Dissolution and Precipitation

As the concentration of the injected geothermal fluid changes over the space and time, silica is dissolved or precipitated into the fracture surface. Figure 3 illustrates the changed in fracture aperture for the reported concentration state in the fracture shown in Figure 2 for the same injection times (15 days and 1 year).

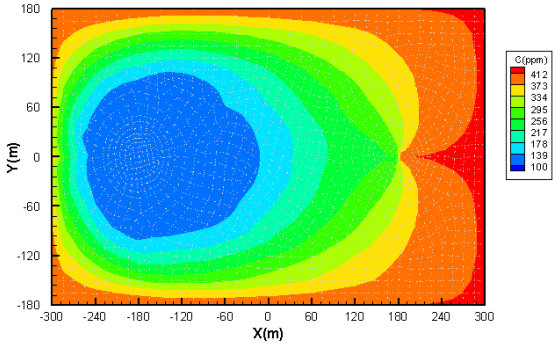

a)

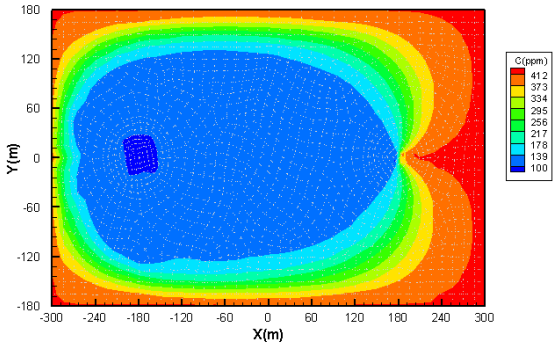

b)

Figure 2: Silica concentration in the fracture after (a) 15 days and (b) 1 year of injection times.

With time, the magnitude of fracture apertures increases (mainly due to silica dissolution), reflecting the contribution of the formation containing quartz. However, silica precipitation occur in a very small region near the injection well where $C>C_{eq}$ due to the fact that the region is cooled to a lower temperature yielding a lower state of equilibrium concentration than its injectate counterpart (this but is not large enough to be readily observable in the plot). Importantly, there exist a band of increasing and decreasing fracture apertures between injection and extraction wells. The maxima occur nearly half way (for injection time of 15 days), but move towards the extraction well (after 1 year in this example). This is because of the varying rates of concentration change (for example, at 15 days of injection time, Figure 5) and reaction (functions of temperature).

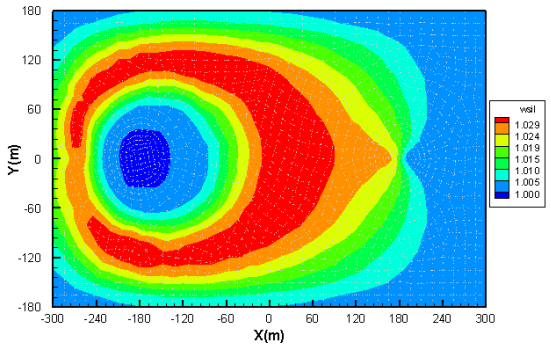

a)

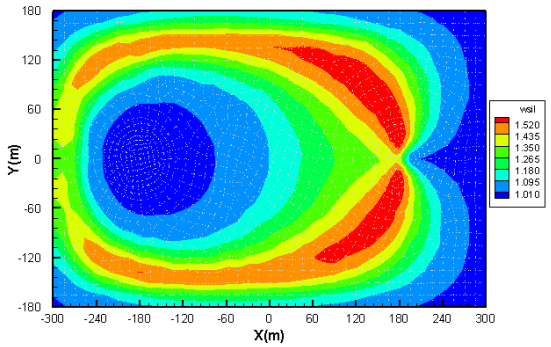

b)

Figure 3: Ratio of the fracture aperture change caused by silica dissolution-precipitation to original aperture after injection time of 15 days (a) and 1 year (b) respectively.

At the extraction well, since the silica concentration decrease with time, the fracture aperture evolves with silica dissolution (see Figure 4). The rate of silica dissolution with respect to time is almost linear, suggesting its linear dependency on the concentration state in the fracture.

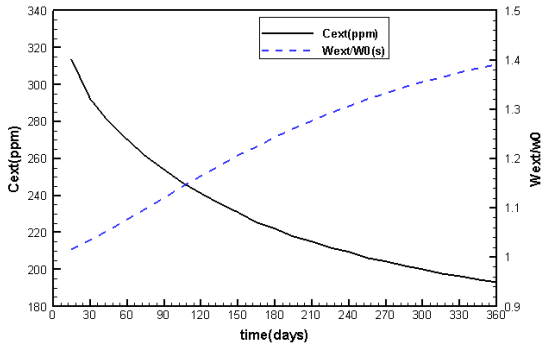

Figure 4: concentration and the effect of silica dissolution on fracture aperture: Extracting fluid concentration (*Left Axis*) and ratio of evolved fracture aperture at extraction well due to dissolution to its initial value (*Right Axis*)

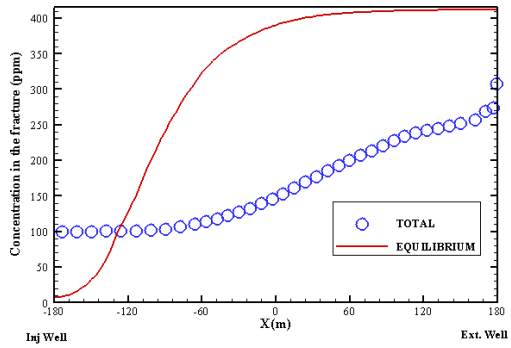

Figure 5: Concentration profile (at o-o) in the fracture at 15 days of injection time.

Pressure and Temperature change

In Figure 6, the induced fluid pressures in the fracture after injecting geothermal fluid for 1 year are plotted. It is observed that the fluid pressure at the injection well has at greater magnitude that at the extraction well. This is because, the extraction well is constrained to be at constant pressure of 17.4 MPa (initial pore-pressure). There is also fluid leak-off from the fracture surface to the rock leading to high pore pressure in the matrix.

The distribution of temperature in the circulating fluid after 1 year of injection time is presented in Figure 7, in which heat depletion has reached the large part of the reservoir with the exception of region beyond to extraction well, and at far in distance. With time, the cooler region expands and moves towards the extraction well, thus there exist a decreasing trend in temperature in the extraction well, showing a declined heat production curve (see Figure 8). The combined effect of thermo- and poro stress on the fracture aperture is also shown in Figure 8, note the increased fracture aperture at the injection well due to large temperature change and pressure increase.

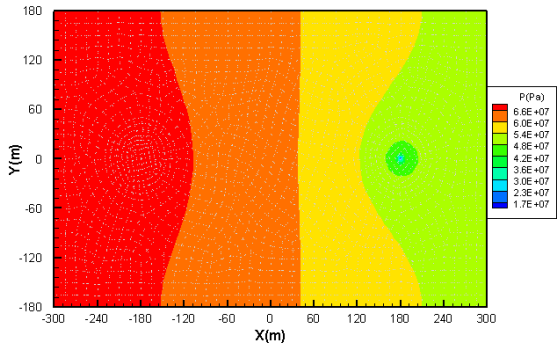

Figure 6: Fluid pressure in the fracture after injection time of 1 year.

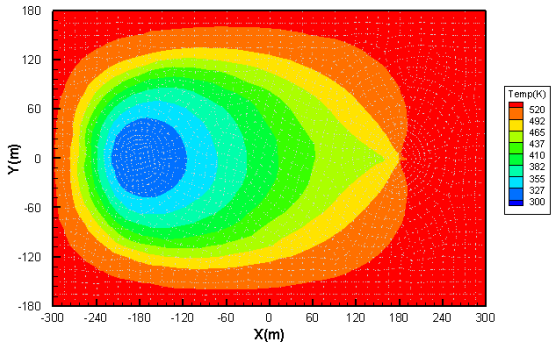

Figure 7: Temperature of the fluid in the fracture after injection time of 1 year.

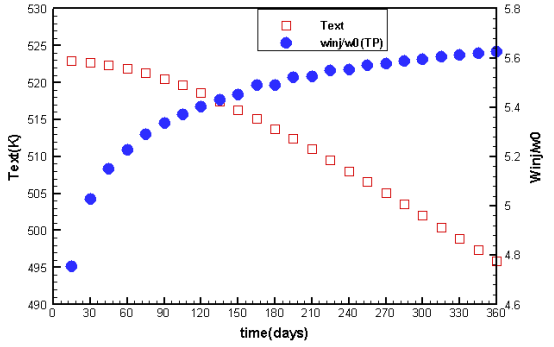

Figure 8: Temperature and the effect of poro-thermo-elastic stress on fracture aperture: Producing fluid temperature (*Left Axis*) and ratio of changed fracture aperture at injection well to its initial value (*Right Axis*)

CONCLUSIONS

We have analyzed reactive flow and poro-thermo-elastic effects of low-temperature fluid injection in a natural fracture using 3D poro-thermo-chemo model. The governing equations of the model were solved using FEM and BEM to investigate fracture aperture change caused by low temperature fluid injection and fluid leak-off into the formation. Both The solute reactivity along the fracture and its diffusion into the rock-matrix are considered using temperature depended reaction kinetics for a single component (silica system).

ACKNOWLEDGEMENTS

This project was supported by the U.S. Department of Energy Office of Energy Efficiency and Renewable Energy under Cooperative Agreement DE-FG36-06GO16059. This support does not constitute an endorsement by the U.S. Department of Energy of the views expressed in this publication. Support of Texas A&M University in publishing this work is also acknowledged.

REFERENCES

Biot, M.A. (1941), "General theory of three-dimensional consolidation", *Journal of Applied Physics*, **12**, 155-164.

Bolton, E.W., Lasaga, A.C., Rye D.M. (1996), "A model for the kinetic control of quartz dissolution and precipitation in porous media flow with spatially variable permeability: Formulation and examples of thermal convection", *Journal of Geophysical Research*, **101**, 22157- 22187.

Brooks A.N., Hughes T.JR. (1982), "Streamline upwind/Petrov-Galerkin formulations for convection dominated flows with particular emphasis on the incompressible Navier-Stokes equations", *Computer Methods in Applied Mechanics and Engineering*, 32,199-259.

Carroll S., Mroczek E., Alai M., Ebert M. (1998), "Amorphous silica precipitation (60 to 120 degrees C): Comparison of laboratory and field rates", Geochim *Cosmochim Acta*, **62,** 1379-1396.

Cheng, AH.-D., Detournay, E. (1998), "On singular integral equations and fundamental solutions of poroelasticity", *International Journal of Solids and Structures*, **35**, 4521–4555.

Cheng, AH.-D., Ghassemi, A. (2001), "Effect of fluid leak-off on heat extraction from a fracture in hot dry rock", *GRC Annual Meeting*.

Cheng, AH.-D., Ghassemi, A., Detournay, E. (2001), "A two-dimensional solution for heat extraction from a fracture in hot dry rock", *International Journal of Numerical and Analytical Methods in Geomechanics*, **25**, 1327-1338.

Dargush, G.F., Banerjee, P.K.(1989), "A time domain boundary element method for poroelasticity", *International Journal for Numerical Methods in Engineering*, **28**, 2423-2449.

Dobson, P.F., Kneafsey, T.J., Sonnenthal, E.I., Spycher, N., Apps J.A. (2003), "Experimental and numerical simulation of dissolution and precipitation: implications for fracture sealing at Yucca Mountain, Nevada", *Journal of Contaminant Hydrology*, **62–63**, 459–476.

Germanovich, L.N., Lowell, R.P. (1992), "Percolation theory, thermoelasticity and discrete

hydrothermal venting in the earth's crust", *Science*, **255,** 1564-1567.

Ghassemi, A., Kumar, S. (2005), "Numerical modeling of non-isothermal quartz dissolution/precipitation in a coupled fracture-matrix system. *Geothermics*, **34**, 411-439.

Ghassemi, A., Kumar, S.(2007), "Changes in fracture aperture and fluid pressure due to thermal stress and silica dissolution/precipitation induced by heat extraction from substrate rocks", *Geothermics*, **36,** 115–140.

Ghassemi, A., Tarasovs, S., Cheng, AH.-D. (2003), "An integral equation solution for three-dimensional heat extraction from planar fracture in hot dry rock", *International Journal for Numerical and Analytical Methods in Geomechanics*, **27,** 989-1004.

Ghassemi, A., Tarasovs, S., Cheng, AH.-D. (2005), "Integral equation solution of heat extraction-induced thermal stress in enhanced geothermal reservoir", *International Journal for Numerical and Analytical Methods in Geomechnics*, **29**, 829-844.

Ghassemi, A., Tarasovs, S., Cheng, AH.-D. (2007), "A 3-D study of the effects of thermomechanical loads on fracture slip in enhanced geothermal reservoirs", *International Journal of Rock Mechanics & Mining Sciences*, **44,** 1132–1148.

Ghassemi, A., Zhang, Q. (2004), "Poro-thermoelastic mechanisms in wellbore stability and reservoir stimulation", *29th Stanford Geothermal Workshop*, Stanford, CA, USA.

Ghassemi, A., Zhou, X.X., (2009), "A Three-dimensional Poro- and Thermoelastic Model for Analysis of Fracture Response in EGS", *Geothermics, to appear*.

Johnson, J.W., Knauss, K.G., Glassley, W.E., DeLoach, L.D., Tompson A.F.B. (1998), "Reactive Transport Modeling of Plug-Flow Reactor Experiments: Quartz and Tuff Dissolution at 240°C", *Journal of Hydrology*, **209,** 81-111.

Lowell, R.P., Cappellen P.V., Germanovich L.N. (1993), "Silica precipitation in fractures and the evolution of permeability in hydrothermal upflow zones", *Science*, **260**, 192-194.

Lowell, R.P., Germanovich L.N.(1994), "On the temporal evolution of high-temperature hydrothermal systems at ocean ridge crests", *Journal of Geophysical Research*, **99,** 565-575.

Martin, T., Lowell, R.P. (1997), "On thermoelasticity and silica precipitation in hydrothermal systems: Numerical modeling of laboratory experiments", *Journal of Geophysical Research*, **102**, 12095-12107.

Rimstidt, J.D. (1979), "The kinetics of silica-water reactions, *PhD Dissertation*, The Pennsylvania State University, USA.

Rimstidt, J.D., Barnes, H.L.(1980), "The kinetics of silica-water reactions", *Geochim Cosmochim Acta*, **44,** 1683-1699.

Robinson, B.A. (1982), "Quartz dissolution and silica deposition in hot dry rock geothermal systems", *Master Thesis*, Massachusetts Institute of Technology, MA, USA.

Robinson, B.A., Pendergrass, J. (1989), "A combined heat transfer and quartz dissolution/deposition model for a hot dry rock geothermal reservoir", Proc. *14th Workshop Geothermal Reservoir Engineering*, Stanford University, Stanford, CA, USA.

Steefel, C.I., Lichtner, P.C. (1998), "Multi-component reactive transport in discrete fractures: I. Controls on reaction front geometry", *Journal of Hydrology*, **209**, 186-199.

Tang, D.H., Frind, E.O., Sudicky E.A. (1981), "Contaminant transport in fractured porous media: analytical solution for a single fracture", *Water Resources Research* 1981, **17-3**, 555-564.

Wangen, M., Munz I.A. (2004), "Formation of quartz veins by local dissolution and transport of silica", *Chemical Geology*, **209**, 179-192.